

OCT 19 1993

OCTI

BERYLLIUM AND GRAPHITE PERFORMANCE IN ITER DURING A DISRUPTION*

A. Hassanein and D.A. Ehst
Argonne National Laboratory
9700 S. Cass Avenue
Argonne, IL 60439 USA

J. Gahl
University of New Mexico
Department of Electrical and
Computer Engineering
Albuquerque, NM 87131 USA

This report was prepared as an account of work sponsored by an agency of the United States Government. Neither the United States Government nor any agency thereof, nor any of their employees, makes any warranty, express or implied, or assumes any legal liability or responsibility for the accuracy, completeness, or usefulness of any information, apparatus, product, or process disclosed, or represents that its use would not infringe privately owned rights. Reference herein to any specific commercial product, process, or service by trade name, trademark, manufacturer, or otherwise does not necessarily constitute or imply its endorsement, recommendation, or favoring by the United States Government or any agency thereof. The views and opinions of authors expressed herein do not necessarily state or reflect those of the United States Government or any agency thereof.

DISCLAIMER

The submitted manuscript has been authored by a contractor of the U. S. Government under contract No. W-31-109-ENG-38. Accordingly, the U. S. Government retains a nonexclusive, royalty-free license to publish or reproduce the published form of this contribution, or allow others to do so, for U. S. Government purposes.

September 1993

* Work supported by the U.S. Department of Energy, Office of Fusion Energy, under Contract W-31-109-Eng-38.

To be presented at the Sixth International Conference on Fusion Reactor Materials, September 27 - October 1, 1993, Stresa, Lago Maggiore, Italy

MASTER

EP

BERYLLIUM AND GRAPHITE PERFORMANCE IN ITER DURING A DISRUPTION*

A. Hassanein and D.A. Ehst
Argonne National Laboratory
9700 S. Cass Avenue
Argonne, IL 60439
U.S.A.

J. Gahl
University of New Mexico
Department of Electrical and
Computer Engineering
Albuquerque, NM 87131
U.S.A.

Abstract

Plasma disruptions are considered one of the most limiting factors for successful operation of magnetic fusion reactors. During a disruption, a sharp, rapid release of energy strikes components such as the divertor or limiter plates. Severe surface erosion and melting of these components may then occur. The amount of material eroded from both ablation and melting is important to the reactor design and component lifetime. The anticipated performance of both beryllium and graphite as plasma-facing materials during such abnormal events is analyzed and compared.

Recent experimental data obtained with both plasma guns and electron beams are carefully evaluated and compared to results of analytical modeling, including vapor shielding effect. Initial results from plasma gun experiments indicate that the Be erosion rate is about five times larger than that for a graphite material under the same disruption conditions. Key differences between simulation experiments and reactor disruption on the net erosion rate, and consequently on the lifetime of the divertor plate, are discussed in detail. The advantages and disadvantages of Be over graphite as a divertor plasma-facing material are discussed.

*Work supported by the U.S. Department of Energy, Office of Fusion Energy, under Contract W-31-109-Eng-38.

1. Introduction

Disruption damage to plasma-facing components in a magnetic fusion reactor is a major concern for component survivability and lifetime evaluation. During a disruption, an intense flow of energy is directed outward from the plasma core to the plasma-facing components. As a result, a sharp deposition of energy ($10\text{-}20\text{ MJ/m}^2$) occurs rapidly ($0.1\text{-}3\text{ ms}$) on components such as the divertor or limiter plates. Severe surface erosion and melting of these components may result. The exact amount of material eroded from both ablation and melting is critically important to reactor design and its component lifetime. In current tokamak machines, ITER - like heat loads and disruption conditions may not be achievable. Therefore, the expected ITER conditions may have to be simulated in laboratory disruption experiments. Experiments using laser light, electron beams, and plasma guns have been used in several countries to study disruption effects on candidate divertor materials [1-5]. The results from these simulation experiments, however, do not generally agree. Recent disruption experiments with plasma guns at the University of New Mexico (USA) and at the Efremov Institute (Russia) reported significantly lower erosion rates than those predicted by theoretical calculations when no shielding effect is taken into account [6,7]. Other Russian experiments with an electron beam on graphite have also shown less erosion than the theoretical predictions, but more erosion than plasma gun experiments under similar simulation conditions [4].

High-Z materials, such as tungsten, are generally expected to have superior performance than low-Z materials, such as beryllium and graphite, regarding both disruption and sputtering erosion in ITER. However, low-Z materials are still favorable from the plasma performance standpoint. The use of Be in JET as a

plasma-facing material has significantly improved plasma performance [8]. Beryllium has mainly increased the density limit, significantly reduced deconditioning after disruptions, and allowed heavy gas fueling for impurity control [9]. Moreover, it has the obvious advantage of lower nuclear charge than graphite. Lower nuclear charge means a lower radiative cooling rate. With graphite limiters, the radiated power in JET plasmas accounted for 30-100% of the input power in which carbon and oxygen contributed most of the radiation. With Be limiters, the radiated power was about 15-60% of the input power, with the lower end of the range being typical [10]. As a result, the use of Be has substantially reduced high-density disruption compared to graphite. However, at higher heating powers, Be plates were very vulnerable to melting which resulted in a rapid deterioration of the discharge due to Be bloom [11]. The highest fusion reaction rate in JET obtained with Be was about half that obtained with carbon. Be plates can, however, withstand higher heating powers when combined with strong gas puffing to increase radiated power [12].

It should be emphasized, however, that most of the advantages associated with Be gettering and fuel pumping, which have significantly improved the performance of JET and reduced the incidence of disruptions, may not be relevant to a machine such as ITER. In a long-pulse device such as ITER, both pumping and gettering will saturate in a time scale that is very short compared to the pulse length. ITER must have effective pumping for impurity control and helium removal.

The anticipated performance of Be and graphite materials during abnormal events such as disruptions is analyzed and compared. Recent experimental data with plasma guns to simulate disruption effects on both Be and graphite is

evaluated and compared to theoretical modeling, including details of vapor shielding effect. Major differences between simulation experiments and disruption conditions in ITER are examined. The overall advantages and disadvantages of using Be over graphite as a plasma-facing material are briefly discussed.

II. Uncertainties in ITER disruption conditions

To evaluate the ITER divertor plate lifetime and net erosion rate, several important factors need to be addressed on plasma conditions at the divertor plate during a disruption. One issue is the plasma-particle kinetic energy during the disruption at the surface of the divertor plate. This energy will determine the penetration depth of the particles in the ablated material and will establish part of the characteristics of the radiation transport through the vapor to the wall. Current estimates of thermal particle kinetic energy during the disruption range from 1 to 20 keV.

Other issues such as geometry of plasma jet striking the divertor surface, angle of incidence, and timing of multiple strikes needs to be investigated. The existence of a sheath potential at the divertor surface during the disruption can, for example, accelerate the plasma particles to energies of about two to three times the presheath incident kinetic energy and may cause more ablation.

Another issue is to determine the partition and the form of the incident energy during the disruption. The disruption energy may be equally partitioned between ions and electrons with the same particle kinetic energy. More disruption energy carried by electrons will probably cause more erosion of the

divertor plate because of their longer range in both the vaporized and condensed divertor material. The disruption may also be preceded by a burst of X-rays. Depending on the amount of energy released as X-rays and on their spectra, this can have affect on the total erosion rate. Other issues such as magnetic field angle of incidence, the reflected energy from the surface, path length of the particles in the vapor, and other edge effects also should be addressed.

III. Simulation experiments versus reactor conditions

Plasma gun experiments used to simulate disruption have mainly used low-energy hydrogen ions ($E < 100$ eV). The plasma-particle kinetic energy in ITER, however, will probably have a much higher energy ($E = 1-20$ keV). Higher particle energy can result in more erosion and a lower vapor shielding effect. A second factor that may exist in the reactor environment but not in plasma gun experiments is the effect of energetic electrons. The plasma energy during a reactor disruption will be partially carried by high energy electrons ($E = 1-20$ keV). Electrons penetrate target materials more deeply than do ions with the same initial particle energy. Vapor shielding is therefore expected to be less effective for electrons than for ions, and the net wall erosion will be higher for electrons than for ions. This is confirmed by recent theoretical modeling and electron beam simulation experiments.

A third factor that can result in a much lower erosion rate in simulation experiments than in reactor conditions is due to the small size of testing specimen samples (area < 5 cm²). In this case, two-and three-dimensional effects of radiation transport above the exposed sample, in the plasma-vapor

interaction zone, can significantly reduce the net radiation flux to the sample and subsequently yield a much lower erosion rate.

On the other hand, an important factor, in the reactor environment which can reduce reactor material erosion rates is the effect of magnetic field. The magnetic field may substantially increase the effectiveness of vapor shielding by increasing the particle path length in the vapor due to the shallow angle between the magnetic field and the divertor wall. Thus, all of the particle kinetic energy and most of the converted radiation energy may be absorbed and reradiated at the outer front of the vapor layer, leaving very little radiation energy to be transported back to the wall and cause significant erosion. However, the inclined nature of the magnetic field lines over the divertor plate can have an adverse effect near the edges of the disruption area where the incoming plasma particles see very little shielding from the eroded materials. As a result, more erosion can be expected near the edges of the disruption area. While the expected energy densities in an ITER disruption ($10\text{-}20\text{ MJ/m}^2$) can be adequately generated by gun experiments, this is not true for disruption time. Most of disruption simulation experiments performed so far have used a deposition time of 0.1 ms. It is very important to conduct disruption experiments with deposition times up to 10 ms to cover the range of the ITER disruption scenario. Vapor shielding may not be as effective in reducing the net erosion rate over longer disruption times. Also, the thickness of the melt layer in metal divertor plates may grow substantially at longer deposition times and become the dominant mechanism in erosion losses.

Besides the usual uncertainties in plasma gun parameters, such as actual calibrated energy deposited on target material, exact time of deposition, and wave form of the gun's power source, other important factors may significantly

affect the accuracy of the modeling and, more important, the relevancy to reactor conditions. One major uncertainty is the amount and type of impurities contained in the gun hydrogen plasma. In some gun experiments, it is believed that the plasma source is dominated by impurities (such as carbon) generated by gun interaction with the Teflon seals of the apparatus [13]. Such uncertainties make modeling efforts and correct interpretation of gun results extremely difficult.

Other factors related to plasma guns that may lead to underestimation of the actual erosion rates include the energy reflected at the target surface, particularly at very low particle energies and the fact that experiments were performed on targets at room temperature. More energy will be reflected at lower particle energies, resulting in less erosion. Higher material temperatures in actual reactor conditions will result in more erosion.

IV. Modeling of gun experiments

A fast and efficient routine has been developed and implemented in the A*THERMAL computer code [14,15] to accurately simulate atomic physics processes due to incoming sub-keV particles typical of plasma gun experiments. Such low-energy particles can suffer 90° scattering and create a thermal plasma source in front of the vaporized target material. In this limit, energy is radiated as photons by the source plasma; this radiation is partly absorbed in the target vapor and partly transmitted through the target material surface. Under typical plasma gun conditions (10 MJ/m², < 1 ms pulse width), the source impulse maintains both the source and target plasmas in the Saha regime. For given densities and vapor temperatures, the code computes the degree of ionization and the effective charge state of both zones. The heat capacity of each vapor,

which can be a significant heat sink in this process, is found from particle kinetic energies, along with the ionization and excitation energy. The source and target plasmas respectively radiate and absorb radiation over a broad spectrum of wavelengths, and the optical depth of each zone is computed at each wavelength by calculating the contributions from Bremsstrahlung (with ions and neutrals) and free-bound radiation. Finally, the equation of radiative transfer determines the photon power spectrum transmitted through the target vapor to the material surface. The code simultaneously solves these equations in a time-dependent manner, conserving energy and following the evolution of the target vapor cloud.

The code also accounts for two-dimensional effects of radiation transport in both the source and the target vapor. The code uses simplified algorithms that eliminate many detailed atomic physics calculations having little bearing on the final result. As a consequence, a fast-running routine is achieved, making parametric studies practical for disruption modeling. Figure 1 shows a simulation example of a hydrogen plasma gun experiment on a Be target. The plasma gun energy density of 12 MJ/m^2 is assumed deposited in 0.1 ms duration. The temperature zones of the plasma gun source and the resulting target vapor are shown as a function of the energy deposition time. The net radiated heat flux to the Be surface from both zones as a result of various atomic physics processes is also shown. This net heat flux becomes substantially lower than the initial unshielded value. Consequently, much lower erosion rates are expected due to the strong shielding of the target vapor.

Fig

Recently, the plasma gun at the University of New Mexico (PLADIS) was used to simulate disruptions on both Be and graphite as well as on other candidate materials. PLADIS is capable of depositing energy densities of up to

Fig

20 MJ/m² in about 100 ms. Figure 2 shows the measured maximum erosion depth for both Be and carbon (POCO graphite) over a range of energy densities at 0.1 ms deposition time. The maximum ablation depth shown was directly measured from recorded surface profilometry. The data points plotted are the average of about 2-3 shots at each energy density. For gun parameters similar to ITER disruption parameters (12 MJ/m² deposited in 0.1 ms), the measured Be erosion loss is about five times higher than that of graphite. One possible reason may be due to loss of the Be melt layer developed during gun-energy deposition. The loss of the melt layer can result from the high pressure associated with plasma gun devices. In reactor environment the loss of melt layer can occur as a result of plasma momentum [16] or by developing instabilities [17].

The average erosion depth inferred from mass loss of Be samples is shown in Fig. 3, along with the maximum erosion depth measured from surface profilometry. Model prediction of eroded Be depth assuming erosion and loss of the melt layer is also shown in Fig. 3. The mass-loss calculations yield an erosion depth that is shallower by a factor of about 2 to 5 than the maximum depth recorded by surface profilometry. Such a discrepancy is not unusual and can be due to factors such as gun beam profile, melt layer movement, and possible redeposited material (particularly near the edges). The model prediction follows the profilometry analysis because the maximum force on the melt layer should be at the center of the sample where the melt layer also peaks. Other plasma gun experiments have also shown substantial erosion rates in materials with high melting rates such as copper and aluminum [18].

Fig 3

Keeping in mind the uncertainties described above for the plasma gun parameters, uncertainties in ITER disruption conditions, and the relevancy of

Fig

plasma gun simulation to reactor conditions, the anticipated disruption lifetime performance of Be and graphite as facing materials is shown in Fig. 4. The maximum number of tolerated disruptions is shown as a function of coating or tile thickness. Because of the high heat load expected during normal operations and the required surface temperature limits, it is assumed that probable initial thicknesses of the Be coating and the graphite tiles are 3 mm and 10 mm respectively. If we assume that 50% of the initial thickness can be sacrificed to disruption erosion, and based the experimental data given in Fig. 2, the predicted disruption lifetime of Be and graphite plasma-facing components are 30 and 500 disruptions, respectively. However, if the heat load on the divertor plate can be reduced by means such as sweeping or gas puffing/radiation cooling methods, the Be coating thickness can then be increased by several millimeters. A 10-mm initial Be coating thickness is expected to survive about 100-full load disruptions.

Use of liquid metals such as lithium (with much higher inlet temperature than water) to cool the divertor will further limit the maximum Be coating thickness required for the same heat flux in order to keep the Be surface temperature at its design limit. A coolant such as NaK, with lower inlet temperature, will allow a thicker Be coating than will the lithium coolant. However, if the divertor plate has to operate at higher surface temperature (350-400° C), required for conditioning purposes between shots, the choice of the coolant will not affect the Be coating thickness. The Be thickness will be decided mainly by the maximum allowable surface temperature and the peak heat load on the divertor plate.

Several other important issues should be considered in the overall erosion comparison between Be and graphite. These issues include sputtering erosion during normal operation, excessive Be melting during longer disruption times,

maximum allowable heat load during normal operation, thermal fatigue associated with pulse operations, and ability to in-situ repair the damaged plasma-facing component. For example, plasma-spraying techniques could be an effective tool in repairing metallic components in-situ rather than replacing damaged graphite tiles.

V. Conclusions

Beryllium and graphite are considered good candidates for plasma-facing materials. The advantages and disadvantages of one material over the other in several major issues related to design, engineering, and operation are rather closely matched. The advantages associated with Be gettering and pumping will not be relevant to long-pulse devices such as the ITER, which will require powerful pumping to control impurities and to remove helium ash. However, in terms of material loss during a disruption, recent plasma gun simulations imply that Be will suffer more erosion than graphite during the same disruption conditions. This is based on limited data available from plasma gun experiments that may not simulate actual reactor disruption conditions. Additional relevant experiments are needed before a final conclusion is made. Furthermore, localized evaporation of Be due to fluctuations in the heat flux will also cause degradation in plasma performance similar to carbon blooms. An additional disadvantage of Be is its vulnerability to melting. Instabilities, erosion, and transport of the melt layer can aggravate this problem.

However, if the use of Be in ITER conditions can reduce the incidence of disruptions compared to graphite performance as proven in JET, the advantage of graphite will then be less obvious. Other important disadvantages of a carbon-

based material are the neutron irradiation effect on its thermophysical properties and the radiation-enhanced sublimation. Neutron irradiation doses as low as 0.1 dpa may significantly reduce the thermal conductivity of carbon and limit its use as a high-heat-flux material. Another concern is the amount of tritium retained in carbon-based materials during operation. However, depending on the conditions of Be surface, large amounts of tritium can also be retained. In addition, the potential to repair a metallic component in-situ by plasma-spraying or other methods may encourage and support the use of Be over nonmetallic materials such as graphite. However, the concern will then be the properties of the plasma-sprayed materials, which may have much lower thermal conductivity that in turn will limit the allowable peak heat load on these materials.

VI. References

- [1] J. Linke et al., J. Nucl. Mater. 196-198 (1992) 607.
- [2] J. G. Van der Laan et al., J. Nucl. Mater. 196-198 (1992) 612.
- [3] H. Bolt et al., Fusion Eng. Des. 18 (1992) 117.
- [4] V.R. Barabash et al., Fusion Eng. Des. 18 (1991) 145.
- [5] M. Seki et al., J. Fusion Energy 5 (1986) 181.
- [6] J. Gahl et al., J. Nucl. Mater. 191-194 (1992) 454.
- [7] A. Hassanein, ASME, 88-WA/NE-2.

- [8] P.H. Rebut et al., IAEA-CN-53/A-I-2 (1991), 27.

- [9] P. Smeulders et al., IAEA-CN-53/A-III-4 (1991), 219.

- [10] P.R. Thomas et al., J. Nucl. Mater. 176 & 177 (1990) 3.

- [11] P.R. Thomas et al., IAEA-CN-53/A-V-3 (1991) 3.

- [12] P.E. Stott et al., J. Nucl. Mater. 196-198 (1992) 3.

- [13] V. Litunovsky, *personal communications*.

- [14] A. Hassanein, J. Nucl. Mater. 122 & 123 (1984) 1453.

- [15] A. Hassanein and D. Ehst, J. Nucl. Mater. 196-198 (1992) 680.

- [16] E. Deksnis et al., J. Nucl. Mater. 176 & 177 (1990) 583.

- [17] A. Hassanein, Fusion Technology 15 (1989) 513.

- [18] J. Linke, *personal communications*.

Figure Captions

- Figure 1. Plasma source and target vapor temperatures and the resulting net radiated heat flux during disruption.
- Figure 2. Maximum ablation depth for Be and graphite measured by surface profilometry.
- Figure 3. Beryllium ablation depth as determined by profilometry (maximum), mass loss (average), and model prediction.
- Figure 4. Maximum tolerated No. of disruptions based on plasma gun results.

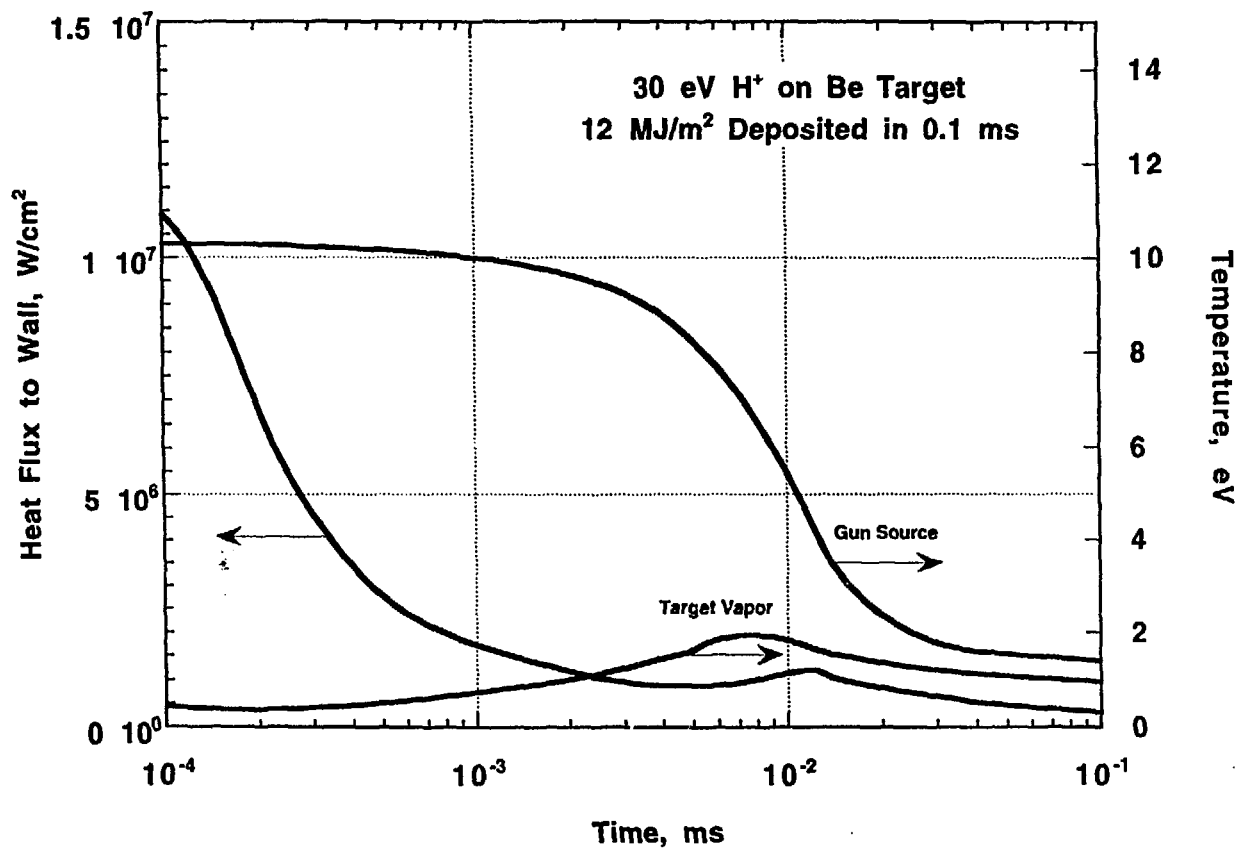


Fig ①

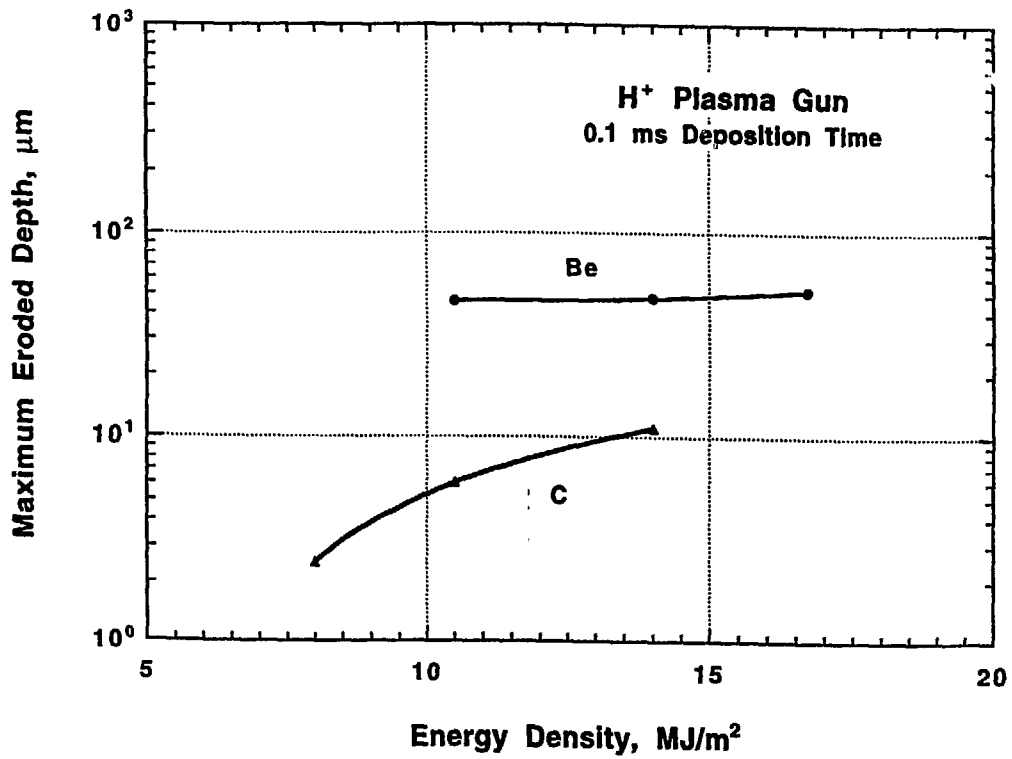


Fig ②

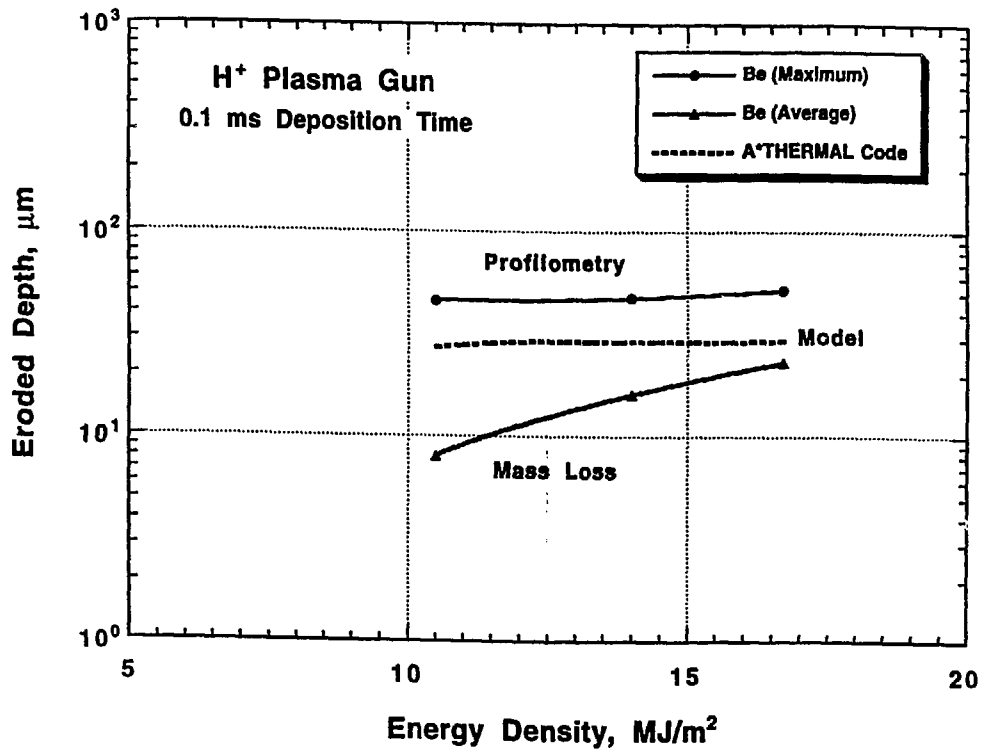


Fig ③

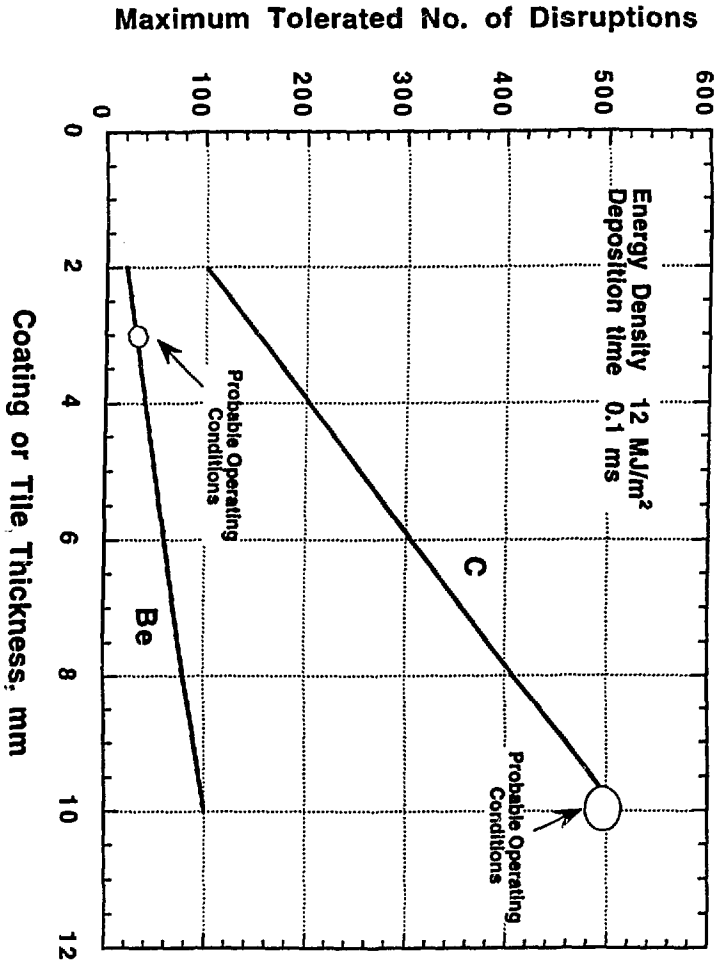


Fig (4)